

Are Small-Scale Deep Convective Clouds in the Tropical Western Pacific Relevant to Intra-Seasonal Oscillations?

*S.A. Barr-Kumarakulasinghe
Marine Sciences Research Center
State University of New York
Stony Brook, New York*

Introduction

Deep convection can occur with convective units on the order of a few kilometers or at large-scale units with cloud sizes on the order of over 100 km in diameter (Figure 1). Studies on convection have typically emphasized large-scale convection. However, the interaction of small-scale and large-scale clouds and the atmosphere is not clear. This analysis demonstrates that the bulk of the areal coverage of cold high-level cloud fluctuates between small and large scale and that this size distribution is well correlated to the upper tropospheric humidity, low level wind, and sea surface temperature (SST) fluctuations. The study also creates a strong inference that the evolution of small-scale clouds to that of large-scale clouds is an integral part of the 30- to 60-day fluctuations in the equatorial atmosphere (Madden Julian Oscillations, MJO) (Madden and Julian 1971).

Data and Methods

The data used in this study were obtained from the public domain and comprise satellite, sounding and analyzed radiation flux data collected during the Tropical Ocean and Global Atmosphere-Coupled Ocean Atmosphere Response Experiment (TOGA-COARE) during November 1992 - February 1993. Cloud statistics were done over the area 152°E-170°E and 6°N-3°S. This region was the location of the 29°C isotherm of SST and covers part of the Inter Tropical Convergence Zone during the November 1992 - February 1993 time period (Figure 2). Humidity and surface wind speeds for this region were considered to be represented by the average obtained from sounding data at Nauru and Kapiangimarangi (Figure 2). Sea surface temperature (SST) for the region was considered to be represented by the 5-m-depth SST data from the TOGA-COARE central mooring (Figure 2). Surface short-wave fluxes were obtained by the International Satellite Cloud Climatology Project (ISCCP) analysis for the region.

Hourly high-level clouds were identified by their infrared (IR) brightness temperature values from the 10-km resolution (GMS-4 IR) images (MRI 1993). Fixed cloud top temperatures were used to demarcate the cloud types. The temperature cutoff for the cold high-level clouds was 223°K (-50°C) and corresponds to an altitude of 12 ± 1 km or at the 200 ± 25 mb, based on the sounding data for Nauru and Kapiangimarangi. Clouds colder than 223°K were searched for in each IR image in the region 152°E, 6°N to 170°E, 3°S and binned according to their contiguous areal coverage in pixels. Areal coverage bin sizes were exponential; clouds less than 2 pixels (~ 100 km²) were not considered in the analysis. The area-size distributions were also converted to an equivalent circular radius in order to calculate changes in perimeter. These hourly results were then averaged to give total and average size of clouds over a day size.

Gill's (1982) empirical formula was used to calculate the saturation vapor pressure (e_s) at each height according to the sounding temperatures at 5-mb intervals at Nauru and Kapiangimarangi. Only soundings at Nauru and Kapiangimarangi were used because these were the only locations for which humidity corrections were made for all soundings during the study period (Parsons et al. 1994).

Results

Under average conditions for the study time period, 50% of the total area covered by high cold clouds was smaller than the $2.56 - 5.12 \cdot 10^4$ km² area size (128-km radius) interval (Figure 3). However, the dominant cloud size oscillated between small and large clouds during the period. During conditions of fair weather typified by Jan 10, the clouds smaller than the $0.320.64 \cdot 10^4$ km² area size (32 - 45 km radius) were over 60% of the total cloud cover. During disturbed weather conditions, high cold clouds larger than the $2.56-5.12 \cdot 10^4$ km² area size interval (90- to 128-km radius) constituted over 70% of the cloud cover. The number of

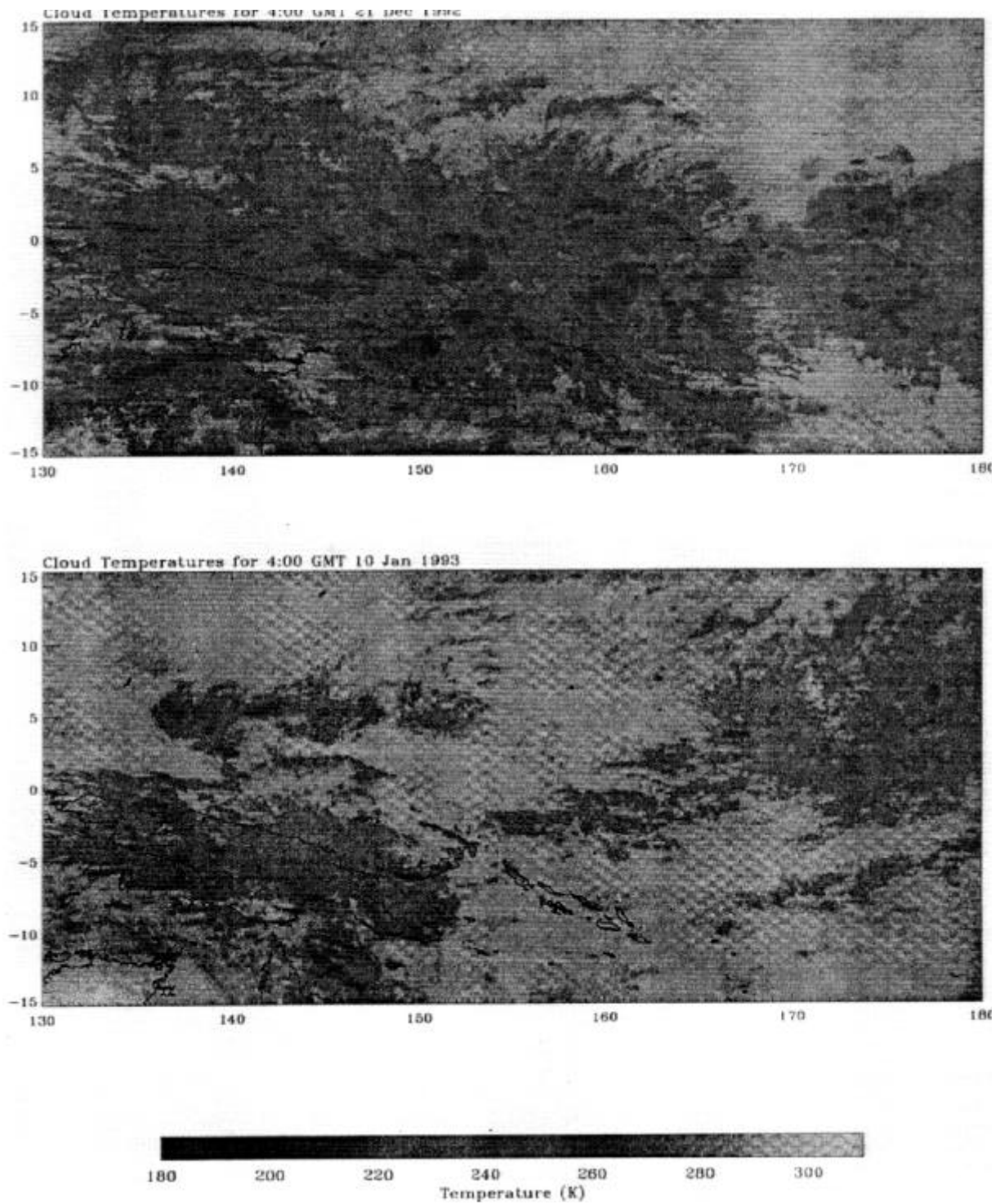


Figure 1. Typical extremes in convective types as seen by GMS-4 infrared imagery. A) 21 December 1992; a day during which mesoscale and large-scale convective clouds have formed and associated with the westerly wind burst. B) 10 January 1993; a day during which small convective elements have formed.

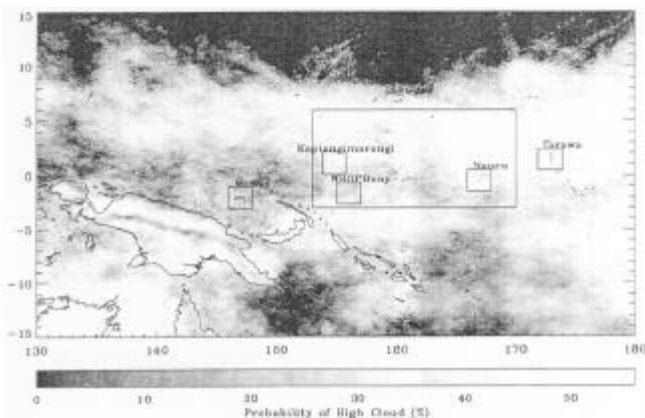


Figure 2. Region of study focus overlaid upon % probability of occurrence of cold high cloud during December 1992 and January 1993.

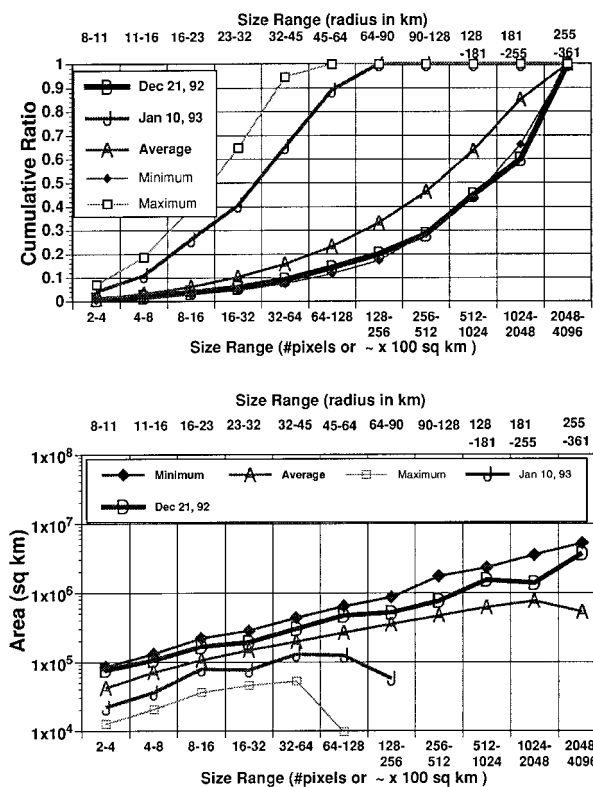


Figure 3. Cumulative cloud size distributions. The average, maximum and minimum for the time period November 1992 - December 1992. Also in the graph are the cumulative distributions for 21 December 1992 and 10 January 1993 which correspond to the days shown in Figure 1.

discrete cold high cloud elements was large for the small sizes and hence causes the average cloud size to be biased toward the lower end of cloud sizes, even though the visual impact is that large clouds predominate (Figure 1).

The average cloud size oscillated in conjunction with the total cloud cover with no lag over the whole period (Figure 4, Table 1). However, just prior to the December storm, total

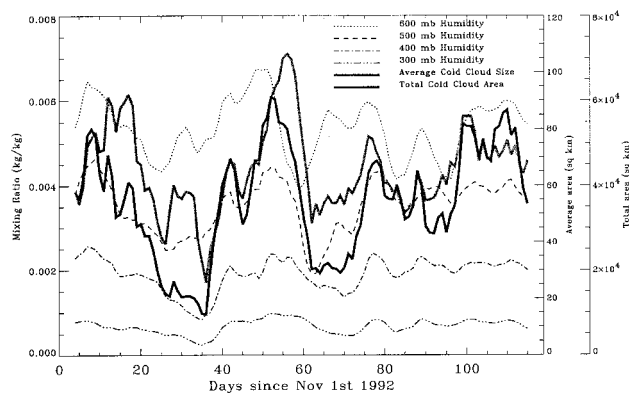


Figure 4. Averaged daily mixing ratios at Nauru and Kapiangimarangi for 600-mb, 500-mb, 400-mb, 300-mb, and 200-mb pressure levels. Also in the diagram are average and total area of cold high cloud. Note that the average size leads total area during the westerly wind burst in December. The data have been smoothed with a 6-day boxcar filter to remove the 3-day variability.

	Slope	r	r ²	Lag ^(a) (days)
Average Size of Cold Cloud	651.82	0.58	0.76	0
SST @ Central Mooring	2.6 x 10 ⁴	0.51	0.71	+30
Surface Insolation	137.60	0.34	0.59	+28
Zonal Wind @ Central Mooring	2.40 x 10 ³	0.14	0.38	+4

(a) Correlations have been done at optimum lag. A positive lag indicates that the parameter follows after the other parameter, e.g., SST maxima occurs 30 days after maximas in surface insolation.

cloud cover precedes average size by about a day. Average high level cloud size for the region and SST at 5-m depth at the TOGA-COARE central mooring were inversely correlated (Figure 5, Table 1). Surface insolation for the region was also inversely correlated with the high cloud size for the region (Figure 5, Table 2). SST followed insolation by three days during the study period (Figure 5, Table 2). Moisture at lower and middle levels of the troposphere leads, and moisture at upper levels follows the cloud size and total area during the study period (Figure 4, Table 3).

Changes in the perimeter of cold high clouds smaller than $2.56 \cdot 10^4 \text{ km}^2$ area size (90-km radius) were strongly correlated with changes in humidity (Figure 6, Table 4). The change in humidity at 500-300 mb preceded the cloud perimeter change by about a day. The regression between humidity and cloud perimeter was strongly correlated and was able to explain 44% of the variance. It is surprising that a large fraction of the variance is explained by the regression between

the change in moisture and the change in cloud perimeter, as only infrared temperatures were used to detect the cold clouds and their sizes and the perimeter calculation assumes circular clouds.

Discussion

This study indicates that often a positive change in humidity precedes an increase in cloud size. This study also shows that high-level small clouds dominate during clear low wind speed conditions and appear to be instrumental in adding moisture to the upper troposphere. This is demonstrated by the increase in moisture that precedes the increase in cloud size. The increase in lower tropospheric humidity prior to the upper troposphere implies a detrainment of humidity by rising convective clouds. Also seen in this analysis is the association of large high-level clouds with lower SSTs. Clear conditions are associated with high SSTs and increased short-wave fluxes.

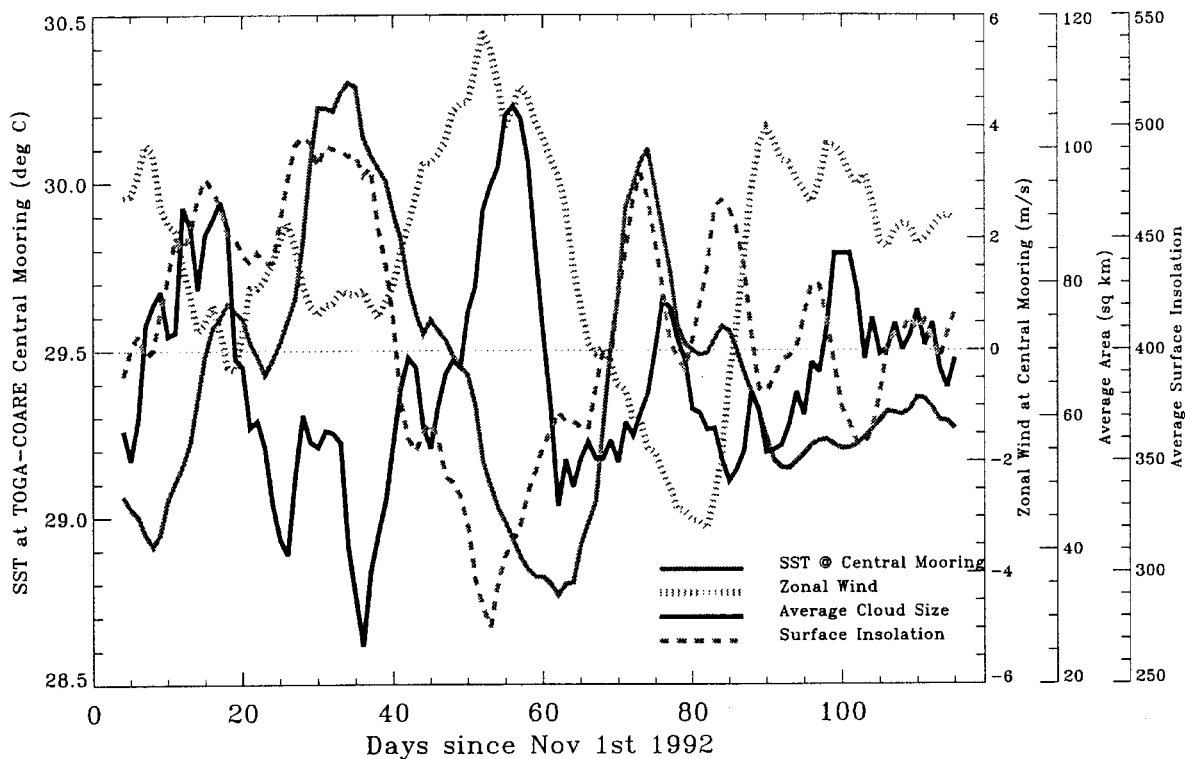


Figure 5. Average size of cold high cloud, SST at 5 m depth, average of zonal wind and surface insolation. The SST and Zonal wind averages are from the TOGA-COARE central mooring data. Surface insolation is for the study region and taken from the ISCCP analysis.

Table 2. Correlation of total area of cold cloud and mixing ratio.

	Interval	Slope	r	r ²	Lag (days)
Mixing Ratio at	600 mb	0.98 x 10 ⁷	0.27	0.52	-2
	500 mb	1.73 x 10 ⁷	0.69	0.83	0
	400 mb	2.87 x 10 ⁷	0.75	0.85	1
	300 mb	6.87 x 10 ⁷	0.74	0.86	1
	200 mb	5.22 x 10 ⁸	0.58	0.76	0

Table 3. Correlation of surface insolation with various parameters.

	Slope	r	r ²	Lag ^(a) (days)
SST @ Central Mooring	0.01	0.54	0.7	3

(a) Correlations have been done at optimum lag. A positive lag indicates that the parameter follows after the other parameter, e.g., SST maxima occurs 3 days after maximas in surface isolation.

Hypothesis

A mechanism has been developed to explain these observations and is shown in Figure 7. Initially the amount and average size of cold high-level clouds are small and associated with high SST and low humidity (Figure 7a). As small cold high-level clouds are generated, they increase the humidity in the overlying atmosphere by detrainment.

This has two consequences. The first is that, given the same amount of perturbation, a larger high-level cloud can be formed as moist energy and instability in the overlying atmosphere increase. Formation of a larger cloud is also facilitated as less detrainment of humidity occurs from the rising air parcel (Walcek 1995). The process of less detrainment is due to a decreased difference in humidity between surrounding environment and a rising air parcel (Walcek 1995; Walcek et al. 1994). The second consequence of having cold high clouds is that solar insolation or short-wave fluxes at the surface decrease, leading to a decrease in SST.

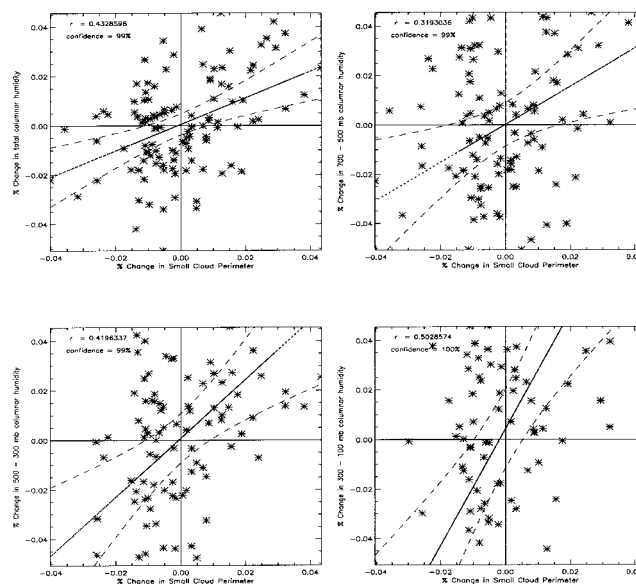


Figure 6. Correlation of change in water vapor within different pressure levels and change in cloud perimeter, a) for total columnar vapor b) 700-500 mb c) 500-300 mb d) 300-100 mb.

Table 4. Correlation of cold cloud perimeter change and columnar humidity.

	Interval	Slope	r	r ²	Lag (days)
Columnar Humidity at	300-100 mb	2.36	0.25	0.50	0
	500-300 mb	1.18	0.17	0.41	-1
	700-500 mb	0.83	0.12	0.34	0
	Total Columnar	0.57	0.22	0.47	0

One of the big questions at this point is, What is the mechanism that causes a perturbation for an air parcel to rise and is it related to SST? This process of increased moisture, increasing cloud size, increasing total cloud cover, and decreasing SST will continue until it culminates in a large storm or westerly wind burst. Two consequences of the large-scale storm are deepening of the ocean mixed layer and removal of the upper tropospheric humidity. The decreased humidity, decreased amount of high-level cloud cover, and deep mixed layer preventing solar radiative fluxes from making their way to the deep water conspire to allow an increase in SST. This brings the system back to approximately the initial state, and the process can be repeated

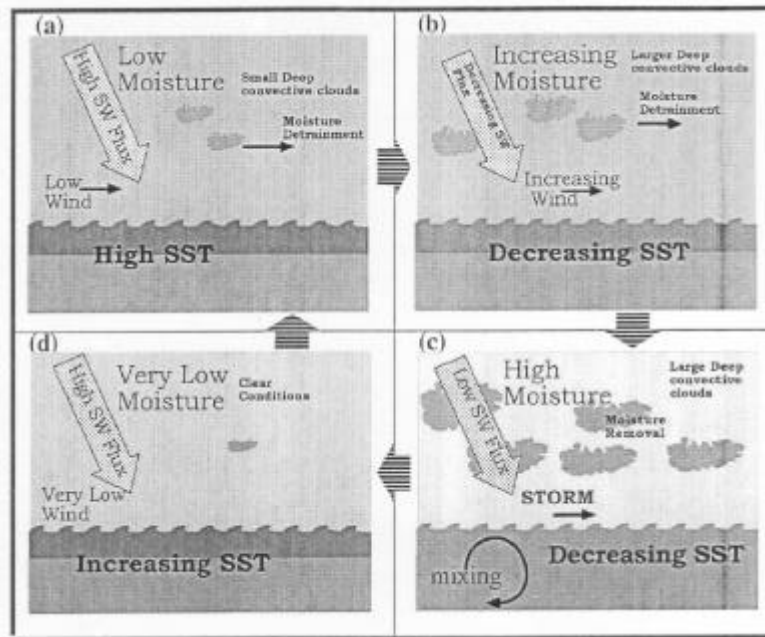


Figure 7. A mechanism for evolution and decay of an intra-seasonal oscillation. The days that are typical of each of the depicted conditions are marked in Figure 4 and Figure 5. A) 35 days after November 1; B) 45 days after November 1; C) 60 days after November 1; D) 65 days after November 1.

if the conditions are right. This is a simple mechanism, but the evolution can be complicated and modified by external conditions such as the advection of warm or cooler waters into the region.

McPhaden et al. (1988) have noted that increased SST or hot spots occur before and after the occurrence of a westerly wind burst. Lien et al. (1995) and Siegel et al. (1995) have observed that increases in SST are the result of the passage of a Kelvin wave and subsequent decrease of turbulent thermal dissipation rates due to deepening of the mixed layer and an increase in light attenuation due to biological activity. McPhaden et al. (1988) has observed that immediately after the westerly wind burst the SSTs are cool due to mixing from below the thermocline and subsequent warming due to advection. This analysis of the evolution of the size scale and total areal cover of cold high clouds in the tropical western Pacific integrates the preceding observations by McPhaden et al. (1988), Lien et al. (1995) and Siegel et al. (1995). An integral part of the explanation is the Walcek hypothesis of moisture detrainment from rising air parcels (Walcek et al. 1994;

Walcek 1995). The study also adds further supporting evidence for detrainment of moisture by an air parcel rising to the surrounding environment. The hypothesis also integrates the observations of Graham and Barnett (1987) and Waliser and Graham (1993) of decreased convective clouds with increasing SST. The observations and hypothesis imply that knowing which mechanisms cause the formation of small-scale convective deep convective clouds may be integral to understanding the variability of the 30- to 60-day fluctuations in the equatorial atmosphere.

References

- Gill, A.E., 1982: Atmosphere-Ocean Dynamics. *International Geophysics Series*, 30. Academic Press, San Diego.
- Graham, N.E., and T.P. Barnett, 1987: Sea Surface Temperature, Surface Wind Divergence, and Convection over the Tropical Oceans, *Nature* **238**:657-659.

Lien, R.-C., D.R. Caldwell, M.C. Gregg, and J.N. Mourn, 1995: Turbulence variability at the equator in the Central Pacific at the beginning of the 1991 - 1993 El-Niño, *J. Geophys. Res.* **100**:6881-6898.

Madden, R., and P.R. Julian, 1971: Detection of a 40-50 day oscillation in the zonal wind in the tropical Pacific. *J. Atmos. Sci.* **28**:702-708.

McPhaden, M.J., H.P. Freitag, S.P. Hayes, B.A. Taft, Z. Chen, and K. Wrytki, 1988: The response of the Equatorial Pacific Ocean to a westerly wind burst in May 1986. *J. Geophys. Res.* **93**:10,589-10,603.

Meteorological-Research-Institute, 1993: GMS-4 Infrared Images over the TOGA-COARE Region. Tokyo, Japan, Japan Meteorological Agency and Science and Technology Agency.

Parsons, D., W. Dabberdt, H. Coloe, T. Hock, C. Martin, A.-L. Barrett, E. Miller, M. Spowart, M. Howard, W. Ecklund, D. Carter, K. Gage and J. Wilson, 1994: The Integrated Sounding System: Description and Preliminary Observations from TOGA-COARE. *Bull. Am. Met. Soc.* **75**:553-567.

Siegel, D. A., C. Ohlmann, L. Washburn, R.R. Bidigare, C. Nosse, E. Fields, and Y. Zhou, 1995: Solar radiation, phytoplankton pigments and the radiant heating of the equatorial Pacific warm pool. *J. Geophys. Res.* **100**:4885-4891.

Walcek, C.J., 1995: Cloud microphysics in GCM cumulus parameterizations: what ensemble-averaged quantities really matter? *AMS Conference on Cloud Physics*, Dallas, Texas, pp: 381-382. American Meteorological Society, Boston, Massachusetts.

Walcek, C.J., Q. Hu, and B. Iacovazzi, 1994: Cumulus clouds parameterized as detraining plumes. *AMS 10th Conference on Numerical Weather Prediction*, Portland, Oregon, pp: 77-78. American Meteorological Society, Boston, Massachusetts.

Waliser, D.E., and N.E. Graham, 1993: Convective Cloud Systems and Warm Pool SSTs; Coupled Interactions and Self Regulation. *J. Geophys. Res.* **98**:12881-12893.

Acknowledgments

This work was supported by an ARM grant to Joyce Tichler, Michael Reynolds, and Peter Minnett. My advisor Kamazima Lwiza's patience and encouragement also made this study possible. Discussions and criticisms from Duane Waliser enhanced and refined this work. Last, but not least, I am extremely grateful to my wife, Chandra, who has supported me in every sense all along.